

Dalton Transactions

Accepted Manuscript



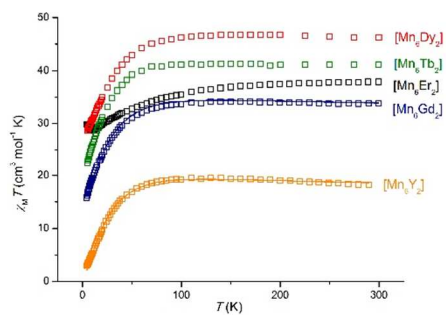
This is an *Accepted Manuscript*, which has been through the Royal Society of Chemistry peer review process and has been accepted for publication.

Accepted Manuscripts are published online shortly after acceptance, before technical editing, formatting and proof reading. Using this free service, authors can make their results available to the community, in citable form, before we publish the edited article. We will replace this *Accepted Manuscript* with the edited and formatted *Advance Article* as soon as it is available.

You can find more information about *Accepted Manuscripts* in the [Information for Authors](#).

Please note that technical editing may introduce minor changes to the text and/or graphics, which may alter content. The journal's standard [Terms & Conditions](#) and the [Ethical guidelines](#) still apply. In no event shall the Royal Society of Chemistry be held responsible for any errors or omissions in this *Accepted Manuscript* or any consequences arising from the use of any information it contains.

A family of octametallic heteronuclear manganese-lanthanide $[\text{Mn}^{\text{III}}_6\text{Ln}_2]$ complexes were isolated and characterized by magnetic measurements.



A family of $[\text{Mn}^{\text{III}}_6\text{Ln}^{\text{III}}_2]$ rod-like clusters

Cite this: DOI: 10.1039/x0xx00000x

 Thomais G. Tziotzi,^a Dimitris A. Kalofolias,^a Demetrios I. Tzimopoulos,^c Milosz Siczek,^d Tadeusz Lis,^d Ross Inglis^{*b} and Constantinos J. Milios^{*a}

 Received 00th January 2012,
 Accepted 00th January 2012

DOI: 10.1039/x0xx00000x

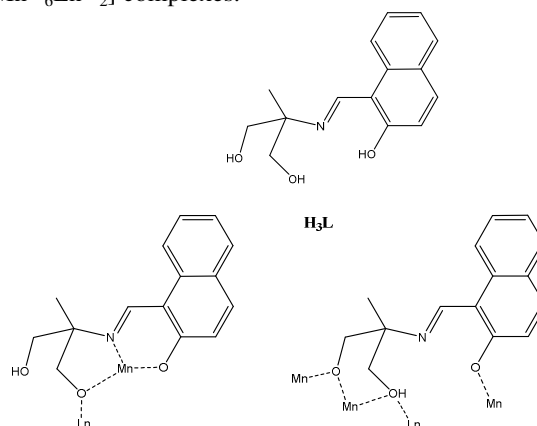
www.rsc.org/

Employment of H_3L (= 2-(β -naphthalideneamino)-2-hydroxymethyl-1-propanol) in mixed-metal manganese-lanthanide cluster chemistry has led to the isolation of five new octametallal heteronuclear isostructural $[\text{Mn}^{\text{III}}_6\text{Ln}^{\text{III}}_2]$ complexes. More specifically, the reaction of $\text{Mn}(\text{ClO}_4)_2 \cdot 6\text{H}_2\text{O}$ with H_3L and the corresponding lanthanide nitrate in MeCN in the presence of base, NEt_3 , yielded five complexes with the general formula $[\text{Mn}^{\text{III}}_6\text{Ln}^{\text{III}}_2\text{O}_2(\text{OH})_2(\text{H}_2\text{O})_2(\text{HL})_6(\text{NO}_3)_6] \cdot 6\text{MeCN} \cdot 0.5\text{H}_2\text{O}$ (Ln: Gd, **1**·6MeCN·0.5H₂O; Tb, **2**·6MeCN·0.5H₂O; Dy, **3**·6MeCN·0.5H₂O; Er, **4**·6MeCN·0.5H₂O). Furthermore, the Y^{III} analogue, $[\text{Mn}^{\text{III}}_6\text{Y}^{\text{III}}_2\text{O}_2(\text{OH})_2(\text{H}_2\text{O})_2(\text{HL})_6(\text{NO}_3)_6] \cdot 6\text{MeCN} \cdot 0.5\text{H}_2\text{O}$ (**5**·6MeCN·0.5H₂O), was also synthesized in the same manner. All five clusters describe a central rod-like topology consisting of four face-sharing defective cubane metallic units, forming a planar hexametallal $[\text{Mn}^{\text{III}}_4\text{Ln}^{\text{III}}_2]$ core, which is further capped by two Mn^{III} ions. Dc magnetic susceptibility studies in the 5 – 300 K range for complexes **1-5** reveal the presence of dominant antiferromagnetic exchange interactions within the metallic clusters, while ac magnetic susceptibility measurements show temperature and frequency dependent out-of-phase signals for the Dy^{III} analogue (**3**·6MeCN·0.5H₂O), suggesting potential single molecule magnetism character. Furthermore, the Y^{III} analogue yielded a diamagnetic ground-state for the $[\text{Mn}^{\text{III}}_6]$ core, thus proving that the SMM character displayed by **3**·6MeCN·0.5H₂O is due to the presence of the Dy^{III} centres.

Introduction

Over the last few years the field of molecular magnetism has been expanding and evolving rapidly into an independent, multi-dynamic field of science and technology; initially involved with the study of the magnetic interactions between the metallic centers within dimeric^[1] and oligonuclear complexes,^[2] witnessed a major boost during the last two decades upon: i) the discovery of polynuclear species that can function as molecular nano-magnets at very low temperatures retaining their magnetization once magnetized in the absence of an external magnetic field, termed as Single Molecule Magnets, SMMs,^[3] and ii) the appearance of analogous behavior in 1D coordination polymers, termed as Single Chain Magnets, SCMs.^[4] Especially in the former case, the compounds that have been found to function as SMMs have grown exponentially; a phenomenon firstly observed for “traditional” transition metal centers like Mn, Fe, Co and Ni,^[3] has now expanded to include 3d-4d/5d, 3d-4f, as well as 4f- and 5f-compounds;^[5] most importantly, the properties of these “new” candidates seem to be very promising towards technological applications, and species with extremely large energy barriers for the re-orientation of the magnetization have been isolated,^[6] given that an Arrhenius analysis is valid for such systems.^[7]

We recently reported the use of the naphthalene-based triol ligand LH_3 (= 2-(β -naphthalideneamino)-2-hydroxymethyl-1-propanol, Scheme 1) in Co(II/III), Ni(II) and Cu(II) chemistry leading to the formation of a $[\text{Co}^{\text{III}}_2\text{Co}^{\text{II}}_3]$, $[\text{Ni}_4]$ and two $[\text{Cu}_4]$ clusters,^[8] and we have now expanded our studies in mixed-metal Mn-Ln chemistry, and herein we report the use of this triol ligand for the synthesis of a family of octanuclear $[\text{Mn}^{\text{III}}_6\text{Ln}^{\text{III}}_2]$ complexes.



Scheme 1. The structure of H_3L and its coordination modes in **1-5**.

Experimental Section

Materials and physical measurements

All manipulations were performed under aerobic conditions, using materials as received. Elemental analyses (C, H, N) were performed by the University of Ioannina microanalysis service. Variable-temperature, solid-state direct current (dc) magnetic susceptibility data down to 2.0 K were collected on a Quantum Design MPMS-XL SQUID magnetometer equipped with a 7 T DC magnet at the University of Edinburgh. Diamagnetic corrections were applied to the observed paramagnetic susceptibilities using Pascal's constants. Powder XRD measurements were collected on freshly prepared samples of 1, 2 and 5 on a PANalytical X'Pert Pro MPD diffractometer at the University of Crete, while EDS measurements were performed on a JEOL Scanning Electron Microscope.

Syntheses

General synthetic strategy applicable to 1-5:

$\text{Mn}(\text{ClO}_4)_2 \cdot 6\text{H}_2\text{O}$ (120.33 mg, 0.33 mmol), $\text{Ln}(\text{NO}_3)_3 \cdot 6\text{H}_2\text{O}$ (0.25 mmol), H_3L (86 mg, 0.33 mmol) and NEt_3 (~ 1 mmol) were dissolved in MeCN (30 mL) forming a yellow suspension that was left upon stirring for ~25' to yield a dark brown solution. The solution was then filtered and left undisturbed to evaporate at room temperature. Dark-brown single-crystals suitable for X-ray crystallography were formed after ~ 2 days in 35-40% yields, and they were washed with Et_2O and dried in air.

Elemental Anal. calcd (found) for **1**:2MeCN: C 40.88 (40.99), H 3.72 (3.53), N 7.10 (7.23); **2**:4MeCN : C 41.39 (41.23), H 3.82 (3.65), N 7.88 (7.76); **3**:2MeCN·0.5H₂O : C 40.75 (40.89), H 3.74 (3.51), N 7.07 (6.98); **4**:3MeCN: C 41.14 (41.01), H 3.77 (3.20), N 7.49 (7.32); **5**:MeCN: C 40.61 (40.53), H 3.66 (3.49), N 6.69 (6.58)%.

X-Ray Crystallography

Diffraction data for **3**:6MeCN·0.5H₂O and **4**:6MeCN·0.5H₂O were collected at 100 K on an Xcalibur PX diffractometer. The structure of Er salt was solved by direct methods. The final atomic parameters of Er crystal were used as starting data for Dy crystal. Both structures were refined by full-matrix least-squares techniques on F^2 with SHELXL.⁹ Data collection parameters and structures solution and refinement details are listed in Table S1. Full details can be found in the CIF files: CCDC 1044737 and 1044738.

Results and Discussion

Syntheses

The reaction between $\text{Mn}(\text{ClO}_4)_2 \cdot 6\text{H}_2\text{O}$ with $\text{Ln}(\text{NO}_3)_3 \cdot 6\text{H}_2\text{O}$ (Ln = Gd, Tb, Dy, Er and Y) and H_3L in 1:0.75:1 ratio in the presence of base, afforded five new heterometallic octanuclear clusters of the $[\text{Mn}^{\text{III}}_6\text{Ln}^{\text{III}}_2\text{O}_2(\text{OH})_2(\text{H}_2\text{O})_2(\text{HL})_6(\text{NO}_3)_6] \cdot 6\text{MeCN} \cdot 0.5\text{H}_2\text{O}$ (Ln: Gd, **1**:6MeCN·0.5H₂O; Tb, **2**:6MeCN·0.5H₂O; Dy, **3**:6MeCN·0.5H₂O; Er, **4**:6MeCN·0.5H₂O; Y, **5**:6MeCN·0.5H₂O) general formulae. The initial synthetic efforts in this reaction system were performed in a 1:1:1 reagents' ratio, but we were not able to isolate any crystalline material, and thus we modified the reaction's stoichiometry. The nature of the base, as well as the presence of

counterions in the reaction mixture, did not affect the identity of the products. We managed to characterize the Gd, Tb, Dy and Er analogues, as well as the Y version, while in the case of larger lanthanide ions we were not able to isolate any crystalline or micro-crystalline material, suggesting that the size of the 4f- ion does affect the formation/stability of the products. For **1-5** we obtained large single-crystals suitable for X-ray crystallography and we chose to solve the representative crystal structures of the Dy (**3**) and Er (**4**) analogues, while the remaining analogues were undoubtedly established by means of IR spectroscopy, PXRD comparison (Figure 1) and elemental analysis. Finally, the purity of the crystalline products was verified by means of energy dispersive spectroscopy, EDS (Figure 2), yielding Mn:Ln ratio of 72.8:27.2, in agreement with the theoretical value of 75:25 as expected for the crystal structure.

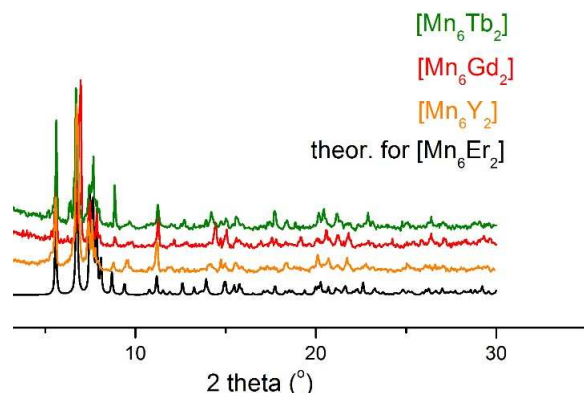


Figure 1. Powder XRD diagrams' comparison for the Tb, Gd and Y analogues, with the theoretical PXRD diagram of the Er analogue.

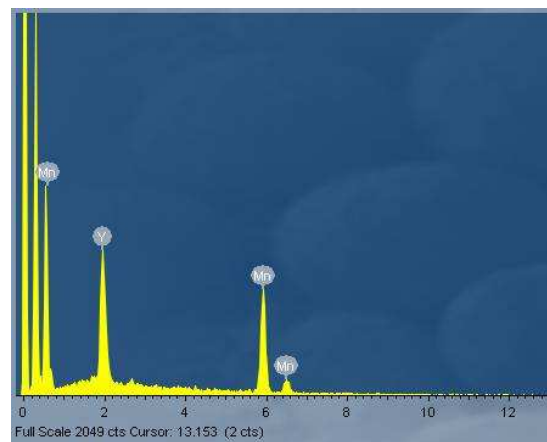


Figure 2. EDS analysis of complex 5.

Description of structures

The molecular structure of complex **3** is presented in Figure 3, while selected interatomic distances and angles for **3** and **4** are given in Table S2 and S3, respectively. Since all crystals are isostructural, we will only discuss the structure of **3**; the compound crystallizes in the triclinic P-1 space group; its structure describes a central planar hexametallate $[\text{Mn}^{\text{III}}_4\text{Ln}^{\text{III}}_2]$ core which is further capped by two Mn^{III} ions. More specifically, Mn1, Mn3, Dy and their symmetry related, form a

central planar $\{\text{Mn}^{\text{III}}_4\text{Dy}^{\text{III}}_2\text{O}_2(\text{OH})_2\}^{12+}$ unit, which is further stabilized by a combination of deprotonated bridging alkoxide groups from the six ligands found in the molecule, and capped by the two “outer” Mn^{III} ions, Mn2 and Mn2'. Four of the six ligands are found in a 2.2101 coordination mode (Harris notation)^[10], with each one forming two chelate rings, while the remaining two are found in a rather unusual 4.2210 mode. Two of the nitrate ions are serving as monoatomic bridges between the central planar core and the capping Mn centres, while the remaining four are bound in a chelate manner on the Dy ions. The coordination environment is further completed by the presence of two terminal H_2O molecules coordinated on Mn3 and Mn3'. All Mn ions are found in the 3+ oxidation state as evidenced by bond valence sum calculations^[11] (BVS: 3.08, 3.10 and 3.14 for Mn1, Mn2 and Mn3, respectively) and are six-coordinate adopting JT distorted octahedral geometry, while the Dy ions are nine-coordinate adopting spherical capped square antiprismatic geometry as calculated from SHAPE.^[12]

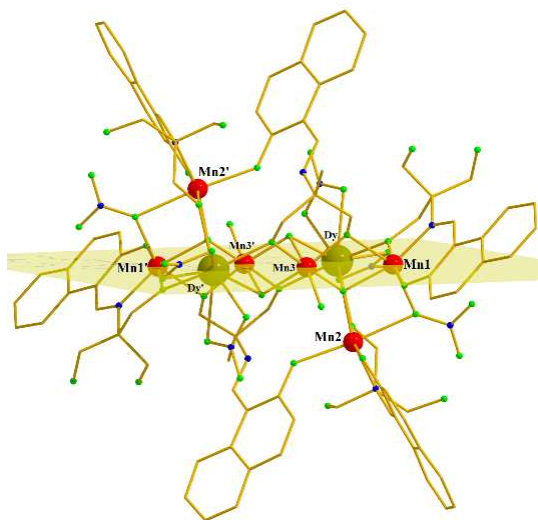


Figure 3. The molecular structure of **3**. Solvent molecules and H atoms are omitted for clarity. Color code: Mn^{III} = red, Dy^{III} = dark-yellow, O=green, N=blue, C=yellow.

There is a number of intra- and intermolecular hydrogen bonds that stabilize the structure of **3** (Figure 4); these H-bonds involve the μ_3 -OH group (O2-H2) which bounds to the alkoxo O1C [O2-H2...O1C (1-x,1-y,1-z) 2.07 Å; O2...O1C 2.813(3) Å; \angle O2-H2...O1C 145°] and the coordinated H_2O molecule (OW1) which bounds to the phenolate O1B atom and to the nitrate O12 atom [OW1-H1W1...O1B 1.95 Å; OW1...O1B 2.789 Å; \angle OW1-H1W1...O1B 165° and OW1-H1W1...O12 1.95 Å; OW1...O12 2.767(4) Å; \angle OW1-H1W1...O12 157°]. In the lattice, the molecules of **3** are also hydrogen-bonded via the pending $-\text{CH}_2\text{-OH}$ groups of the ligand to form a chain running parallel to the a axis. In this arrangement, each molecule of **3** participates in four H-bonds [one unique: O15B-H15B...O15A (x-1,y,z) 1.92 Å; O15B...O15A 2.780(5) Å; \angle O15B-H15B...O15A 176°], while the second pending $-\text{CH}_2\text{-OH}$ group is attached to a CH_3CN molecule [O15A-H15D...N5 1.88 Å; O15A...N5 2.753(6) Å; \angle O15A-H15A...N5 177°]. Several weaker intra- and intermolecular C-H...O interactions are also present, while besides the presence of several phenyl groups there are not any π - π interactions. Complexes **1-5** join only a handful of structurally characterized $[\text{Mn}_6\text{Ln}_2]$ complexes.^[13]

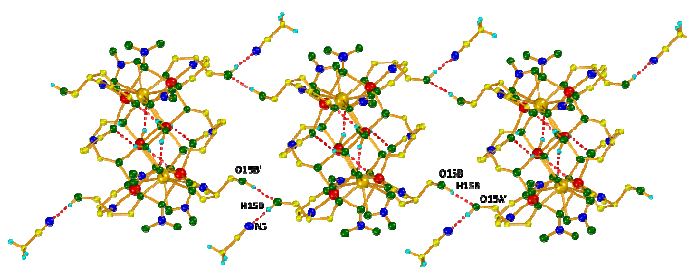


Figure 4. The hydrogen-bonded chain of **3** along a . Dashed-red lines represent hydrogen bonds. Symmetry codes: (') 1+x, y, z; (')' x-1, y, z. Color code: same as in Fig.3

Magnetochemistry

Dc Magnetic Susceptibility Studies

Direct current magnetic susceptibility studies were performed on polycrystalline samples of **1-5** in the 5 – 300 K range under an applied field of 0.1 T. The results are plotted as the $\chi_M T$ product vs. T in Figure 5. From a quick glance at Figure 5, we can clearly see that all complexes display similar behaviour, *i.e.* the $\chi_M T$ product decreases upon cooling, suggesting the presence of dominant antiferromagnetic interactions, although this statement is risky due to the simultaneous depopulation of the Stark sub-levels (for complexes **2**, **3** and **4**). For all five $[\text{Mn}_6\text{Ln}_2]$ complexes the room temperature $\chi_M T$ values were found very close to the theoretical $\chi_M T$ values expected for six non-interacting Mn^{III} ions ($g = 2.00$) and two Ln^{III} ($\text{Ln} = \text{Gd}$, **1**; Tb , **2**, Dy , **3**; Er , **4**; Y , **5**) ions with their corresponding g_i values ($g_{\text{Gd}} = 2.00$, $g_{\text{Tb}} = 1.50$, $g_{\text{Dy}} = 1.33$ and $g_{\text{Er}} = 1.20$). More specifically, for complex **1**, the room temperature $\chi_M T$ value of $33.73 \text{ cm}^3 \text{ mol}^{-1} \text{ K}$ (theoretical value of $33.75 \text{ cm}^3 \text{ mol}^{-1} \text{ K}$) remains unchanged upon cooling until ~ 100 K, before it drops to its minimum value of $15.81 \text{ cm}^3 \text{ mol}^{-1} \text{ K}$ at 5 K. For complex **2** the room temperature $\chi_M T$ value of $41.16 \text{ cm}^3 \text{ mol}^{-1} \text{ K}$ (theoretical value of $41.62 \text{ cm}^3 \text{ mol}^{-1} \text{ K}$) remains constant upon cooling until ~ 90 K, before it drops to the minimum value of $22.34 \text{ cm}^3 \text{ mol}^{-1} \text{ K}$ at 5 K. Complex **3** displays analogous behaviour; the room temperature $\chi_M T$ value of $46.14 \text{ cm}^3 \text{ mol}^{-1} \text{ K}$ (theoretical value of $46.31 \text{ cm}^3 \text{ mol}^{-1} \text{ K}$) remains constant upon cooling until ~ 100 K, before it drops to

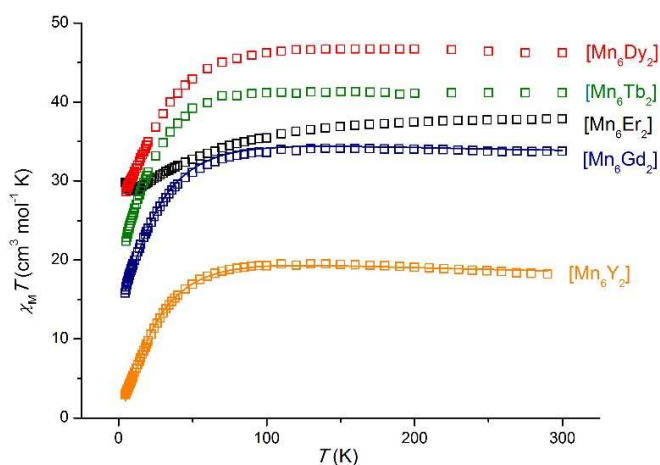


Figure 5. $\chi_M T$ vs. T plot for complexes **1** ($[\text{Mn}_6\text{Gd}_2]$), **2** ($[\text{Mn}_6\text{Tb}_2]$), **3** ($[\text{Mn}_6\text{Dy}_2]$), **4** ($[\text{Mn}_6\text{Er}_2]$) and **5** ($[\text{Mn}_6\text{Y}_2]$) under an applied *dc* field of 1000 G. The solid lines represent fit of the data in the 5 – 300 K (see text for details).

the minimum value of $28.62 \text{ cm}^3 \text{ mol}^{-1} \text{ K}$ at 5 K. The Er analogue (**4**) displays slightly different behaviour; the room

temperature $\chi_M T$ value of $38.83 \text{ cm}^3 \text{ mol}^{-1} \text{ K}$ (theoretical value of $40.95 \text{ cm}^3 \text{ mol}^{-1} \text{ K}$) remains constant upon cooling until $\sim 150 \text{ K}$ below which it decreases to reach the minimum value of $28.68 \text{ cm}^3 \text{ mol}^{-1} \text{ K}$ at 10 K , while upon further cooling it slightly increases to reach the value of $29.87 \text{ cm}^3 \text{ mol}^{-1} \text{ K}$. Finally, for the “diamagnetic” analogue **5** the room temperature $\chi_M T$ value of $18.16 \text{ cm}^3 \text{ mol}^{-1} \text{ K}$ (theoretical value of $18.00 \text{ cm}^3 \text{ mol}^{-1} \text{ K}$) increases slightly upon cooling to reach the maximum value of $19.30 \text{ cm}^3 \text{ mol}^{-1} \text{ K}$ at $19.49 \text{ cm}^3 \text{ mol}^{-1} \text{ K}$ at 110 K , below which it decreases to its minimum value of $2.92 \text{ cm}^3 \text{ mol}^{-1} \text{ K}$ at 5 K . In order to get a qualitative view of the dominant interactions present in each cluster we performed a Curie-Weiss analysis of the high-temperature ($50 - 300 \text{ K}$) magnetic susceptibility data (Figure 6) yielding θ values of -2.06 K , -0.95 K , -1.71 K , -10.04 K and 2.60 K , for **1**, **2**, **3**, **4** and **5**, respectively.

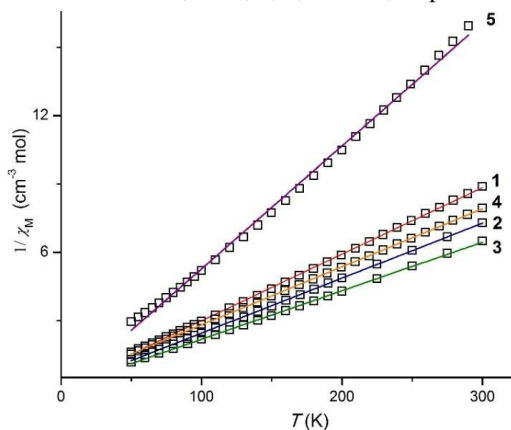


Figure 6. Curie-Weiss plot for complexes **1-5** for the $50 - 300 \text{ K}$ temperature range.

We were able to successfully fit the $\chi_M T$ data for the $[\text{Mn}_6\text{Y}_2]$ cluster (**5**) adopting a 2- J model (Figure 7, top) and the Hamiltonian equation (1), which assumes the following exchange interactions: one exchange, J_1 , between i) Mn2-Mn3 (and Mn2'-Mn3') mediated by one oxo bridge with Mn-O-Mn angle of $\sim 132^\circ$, ii) Mn1-Mn2 (and Mn1'-Mn2') mediated by an oxo bridge (Mn-O-Mn: 109.6°) and by a monoatomic nitrate bridge (Mn-O-NO₃-Mn: 90.3°) and iii) between Mn3-Mn3' mediated by two hydroxide bridges (Mn-O(H)-Mn: 102.8°), and one J_2 between Mn1-Mn3 (and Mn1'-Mn3') mediated by one oxo bridge (Mn-O-Mn: 101.3°) and one monoatomic alkoxide bridge (Mn-O(R)-Mn: 100.8°). Using the powerful program PHI,^[14] and employing the Hamiltonian in eqn (1)

$$\hat{H} = -2J_1 (\hat{S}_3 \hat{S}_2 + \hat{S}_3' \hat{S}_2' + \hat{S}_1 \hat{S}_2 + \hat{S}_1' \hat{S}_2' + \hat{S}_3 \hat{S}_3') - 2J_2 (\hat{S}_1 \hat{S}_3 + \hat{S}_1' \hat{S}_3') \quad (1)$$

afforded the parameters $J_1 = -1.46 \text{ cm}^{-1}$, $J_2 = 11.09 \text{ cm}^{-1}$ and $g = 1.97$. These parameters lead to an $S = 0$ ground-state, with the first excited state of $S = 1$ located only 1.2 cm^{-1} above. The ferromagnetic nature of J_2 is in good agreement with previously reported “out-of-plane” $[\text{Mn}^{\text{III}}(\text{OR})_2]^{4+}$ units.^[15] Finally, the system may be treated as two antiferromagnetically coupled $S = 2$ triangles. In Figure 8, the plot of the relative error surface for fitting the data for **5** as a function of J_1 and J_2 is shown, following the sum of squares approach and by using PHI;^[14] the J values obtained belong to

a well-defined minimum for this system in the $\{-2.5, -1.6\}$ (for J_1) $\{-8.4, 13.5 \text{ cm}^{-1}\}$ (for J_2) region, with J_1 deviating only by 0.14 cm^{-1} .

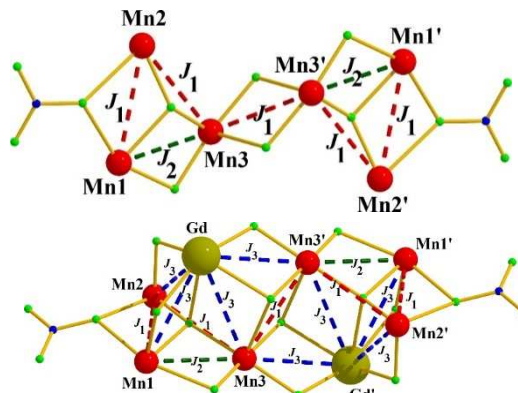


Figure 7. Exchange interaction scheme for complexes **5** (top) and **1** (bottom); see text for details.

Using exactly the same parameters found for **5**, we were able to successfully fit the $\chi_M T$ data for the $[\text{Mn}_6\text{Gd}_2]$ cluster (**1**) by simply adding the exchange interaction J_3 between the Mn^{III} - Gd^{III} ions, retaining the J_1 and J_2 values as found in **5**. Therefore, adopting the 3- J model (Figure 7, bottom) and the Hamiltonian in eqn (2)

$$\hat{H} = -2J_1 (\hat{S}_3 \hat{S}_2 + \hat{S}_3' \hat{S}_2' + \hat{S}_1 \hat{S}_2 + \hat{S}_1' \hat{S}_2' + \hat{S}_3 \hat{S}_3') - 2J_2 (\hat{S}_1 \hat{S}_3 + \hat{S}_1' \hat{S}_3') - 2J_3 (\hat{S}_1 \hat{S}_{\text{Gd}} + \hat{S}_2 \hat{S}_{\text{Gd}} + \hat{S}_3 \hat{S}_{\text{Gd}} + \hat{S}_1' \hat{S}_{\text{Gd}'} + \hat{S}_2' \hat{S}_{\text{Gd}'} + \hat{S}_3' \hat{S}_{\text{Gd}'}) + \hat{S}_3 \hat{S}_{\text{Gd}} + \hat{S}_3' \hat{S}_{\text{Gd}'} \quad (2)$$

yielded $J_3 = -0.07 \text{ cm}^{-1}$ with all other parameters as in **5**, with $g_{\text{Mn}} = 1.97$ and $g_{\text{Gd}} = 2.00$, leading to the $S = 0, 1, 2, 3, 4, 5, 6$ and 7 spin-states located within less than 0.1 cm^{-1} . Most importantly, we obtained exactly the same J_1 , J_2 and J_3 parameters upon performing a “free” fit of the data, without “locking” the J_1 and J_2 values, proving the correctness of our method. Such weak, either ferro- or antiferromagnetic, Mn-Gd interactions (J_3 in our case) have been reported previously in related systems,^[16] and are well expected due to the inner nature of the $4f$ electrons. The influence of the J_3 interaction, albeit weak, can be seen in Fig. S1, where the plot of the difference between the $\chi_M T_{[\text{Mn}_6\text{Gd}_2]} - \chi_M T_{[\text{Mn}_6\text{Y}_2]}$ vs. T is presented.

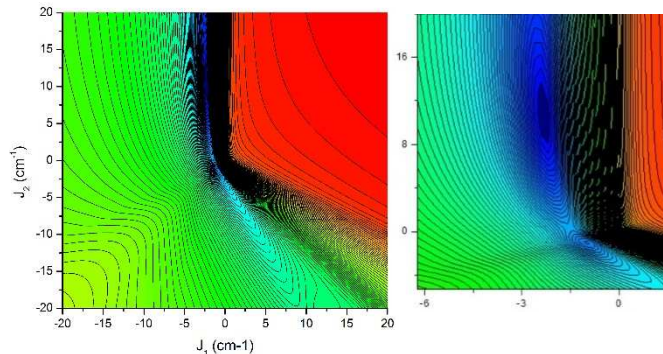


Figure 8. (Left) 2D-contour plot of the relative error surface for fitting the magnetic data of **5**; (right) zoom-in view of the 2D-contour plot, showing the $\{-2.5, -1.6\}J_1$ $\{-8.4, 13.5 \text{ cm}^{-1}\}J_2$ region (dark-blue).

Furthermore, magnetization data were collected for **1** in the magnetic field and temperature ranges of 1 – 7 T and 2.0 – 7.0 K, but a good fit for the reduced magnetization data was not possible assuming that only the ground state is populated, as was already evidenced by the dc magnetic susceptibility fit. Still, we managed to successfully simulate the M vs. H data with the parameters obtained from the dc susceptibility fit (Figure 9).

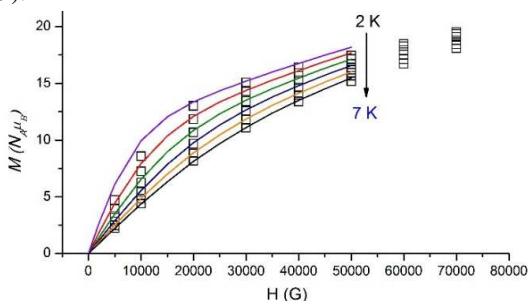
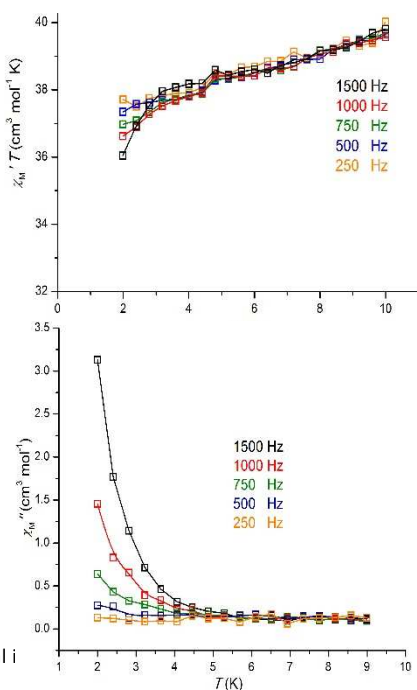


Figure 9. M vs. H for **1** in the 1 – 7 T and 2.0 – 7.0 K field and temperature range. The solid lines represent simulation of the magnetization isotherms in the 1-5 T field range and 2-7 K temperature range (top-to-bottom), assuming the parameters obtained from the dc susceptibility simulation (see text for details).

Ac Magnetic Susceptibility Studies

Ac magnetic susceptibility measurements were performed on polycrystalline samples of all **1-5** complexes, in the 1.8 – 10 K range in zero applied dc field and 3.5 G ac field oscillating at 100 – 1500 Hz range, as a means of investigating possible SMM behaviour. From all complexes studied, only cluster **3**, $[\text{Mn}_6\text{Dy}_2]$ displayed interesting behaviour; the in-phase, χ_M' , (plotted as $\chi_M' T$ vs. T , Figure 10, top) signal decreases upon decreasing temperature, indicating the presence of low-lying excited states with higher “ S ” values than the ground-state. Furthermore, it displays frequency-dependent out-of-phase, χ_M'' , signals below ~ 4 K, but no peaks are seen (Figure 10, bottom), indicating the possibility of SMM behaviour, albeit with a small barrier to magnetization reversal.



This journal i

Figure 10. Plot of the in-phase (χ_M') signal as $\chi_M' T$ vs. temperature for complex **3** (top); plot of the out-of-phase χ_M'' signal vs. temperature for complex **3** (bottom).

Since: i) the Y^{III} analogue, cluster **5**, is diamagnetic and as such does not display SMM behavior, and ii) the Dy^{III} shows SMM characteristics, we can safely assume that the replacement of the Y^{III} ions with the Dy^{III} ions led to an increase of the “ground-state” and an increase of the magnetic anisotropy present. Given that in the absence of high symmetry, the ground-state of Dy^{III} ions is a doublet along the anisotropy axis with $m_J = \pm 15/2$,^[17] we were able to calculate the anisotropy axis for each Dy^{III} ion using a simple, and yet genius, electrostatic model recently reported by Chilton *et al.*, based on electrostatic energy minimization for the prediction of the ground state magnetic anisotropy axis.^[18] Following this method and program MAGELLAN, the ground state magnetic anisotropy axes for each Dy center in **3** was found tilted towards the O2 atom belonging to the hydroxide group connected on the lanthanide center, and towards O21 belonging to the bidentate NO_3^- anion (Figure 11, left). Finally, the two axes of **3** were found co-parallel since the two ions are related by inversion symmetry (Figure 11, right).

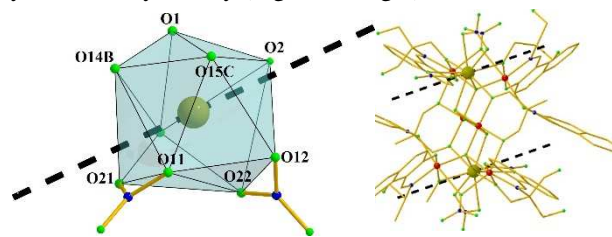


Figure 11. (Left) Ground state magnetic anisotropy axis for the Dy center present in **3**; (right) parallel orientation of the two magnetic anisotropy axis of the Dy^{III} ions in **3**.

Conclusions

In conclusion, we have reported the syntheses, structures, and magnetism of five octametallate heteronuclear $[\text{Mn}^{\text{III}}_6\text{Ln}_2]$ clusters upon employment of the (2-(β -naphthalideneamino)-2-hydroxymethyl-1-propanol) ligand, LH_3 . Following our results upon employment of LH_3 in $\text{Co}(\text{II/III})$, $\text{Ni}(\text{II})$ and $\text{Cu}(\text{II})$ chemistry,^[8] we have now found that this versatile ligand can also lead to beautiful 3d-4f structures with interesting magnetic properties. Work is currently underway in order to investigate and isolate more examples of 3d-4f species, from analogous systems.

Acknowledgements

CJM would like to thank The Excellence Grant (ARISTEIA-2691) for funding. RI would like to thank The Royal Society of Edinburgh for funding. DIT would like to thank the 89439/2012 Grant of the Aristotle University of Thessaloniki.

Notes and references

^a Department Of Chemistry, University of Crete, Voutes 71003, Herakleion, Greece. Fax: +30-2810-545001; Tel: +30-2810-545099; E-mail: kamil@chemistry.uoc.gr

^b School of Chemistry, The University of Edinburgh, David Brewster Road, EH9 3FJ, Edinburgh, UK. Tel: +44-131-6507545; Email: ringlis@staffmail.ed.ac.uk

^c Department of Chemistry, Aristotle University of Thessaloniki, 54124, Thessaloniki, Greece.

^d Faculty Of Chemistry, University of Wroclaw, Joliot-Curie 14, Wroclaw 50-383, Poland.

† Footnotes should appear here. These might include comments relevant to but not central to the matter under discussion, limited experimental and spectral data, and crystallographic data.

Electronic Supplementary Information (ESI) available: [details of any supplementary information available should be included here]. See DOI: 10.1039/b000000x/

- 1 See for example: B. Bleaney and K. D. Bowers, *Proc. Roy. Soc. London*, 1952, **A214**, 451; M. Kato, H. B. Jonassen and J. C. Fanning, *Chem. Rev.*, 1963, **64**, 99; W. H. Crawford, H. W. Richardson, J. R. Wasson, D. J. Hodgson and W. E. Hatfield, *Inorg. Chem.*, 1976, **15**, 2107; W. E. Hatfield, *Comments Inorg. Chem.*, 1981, **1**, 105; M. F. Charlot, O. Kahn and M. Drillon, *Chem. Phys.*, 1982, **70**, 177; D. J. Hodgson, In *Magneto-Structural Correlations in Exchange Coupled Systems*; D. Gatteschi, O. Kahn and R. D. Willett, Eds.; D. Reidel: Dordrecht, 1985; pp 497-522; A. Bencini, C. Benelli, A. Caneschi, R. L. Carlin, A. Dei and D. Gatteschi, *J. Am. Chem. Soc.*, 1985, **107**, 8128; C. Benelli, A. Caneschi, D. Gatteschi, O. Guillou and L. Pardi, *Inorg. Chem.*, 1990, **29**, 1750; O. Kahn, *Molecular Magnetism*, VCH, New York, 1993; S. S. Tandon, L. K. Thompson, M. E. Manuel and J. N. Bridson, *Inorg. Chem.*, 1994, **33**, 5555; S. M. Gorun and S. J. Lippard, *Inorg. Chem.*, 1991, **30**, 1625; M. Melnik, *Coord. Chem. Rev.*, 1982, **42**, 269; M. Kato and Y. Muto, *Coord. Chem. Rev.*, 1988, **92**, 45.
- 2 Representative refs and refs therein: T. Cauchy, E. Ruiz and S. Alvarez, *J. Am. Chem. Soc.*, 2006, **128**, 15722; F. Neese, *J. Am. Chem. Soc.*, 2006, **128**, 10213; M. R. Pederson and S. N. Khanna, *Phys. Rev. B*, 1999, **59**, 693; A. V. Postnikov, J. Kortus and M. R. Pederson, *Physica Status Solidi (b)*, 2006, **243**, 2533; M. A. Halcrow, J.-S. Sun, J. C. Huffman and G. Christou, *Inorg. Chem.*, 1995, **34**, 4167.
- 3 For reviews concerning the “first era” of SMMs, see: G. Aromi and E. K. Brechin, *Struct. Bonding*, 2006, **122**, 1; R. Bircher, G. Chaboussant, C. Dobe, H. U. Güdel, S. T. Ochsenein, A. Sieber and O. Waldman, *Adv. Funct. Mater.*, 2006, **16**, 209; D. Gatteschi and R. Sessoli, *Angew. Chem., Int. Ed.*, 2003, **42**, 268; G. Christou, D. Gatteschi, D. N. Hendrickson, and R. Sessoli, *MRS Bull.*, 2000, **25**, 66.
- 4 See for example: A. Caneschi, D. Gatteschi, N. Lalioti, C. Sangregorio, R. Sessoli, G. Venturi, A. Vindigni, A. Rettori, M. G. Pini and M. A. Novak, *Angew. Chem., Int. Ed.*, 2001, **40**, 1760; R. Clérac, H. Miyasaka, M. Yamashita and C. Coulon, *J. Am. Chem. Soc.*, 2002, **124**, 12837; L. Bogani, A. Vindigni, R. Sessoli and D. Gatteschi, *J. Mater. Chem.*, 2008, **18**, 4750; C. Coulon, H. Miyasaka and R. Clérac, *Struct. Bonding*, 2006, **122**, 163; H. Miyasaka and M. Yamashita, *Dalton Trans.*, 2007, 399; H.-L. Suna, Z.-M. Wang and S.

- Gao, *Coord. Chem. Rev.*, 2010, **254**, 1081; W.-X. Zhang, R. Ishikawa, B. Breedlove and M. Yamashita, *RSC Adv.*, 2013, **3**, 3772; D. Gatteschi and A. Vindigni, *Molecular Magnets* in “Nanoscience and Technology” book series, Eds. J. Bartolomé, J. F. Fernández and F. Luis, Springer-Verlag: Berlin Heidelberg, 2014; C. Coulon, Vivien Pianet and R. Clérac, *Struct. Bonding*, 2014, DOI: 10.1007/430_2014_154; R. Lescouëzec, J. Vaissermann, C. Ruiz-Pérez, F. Lloret, R. Carrasco, M. Julve, M. Verdaguer, Y. Dromzee, D. Gatteschi and W. Wernsdorfer, *Angew. Chem. Int. Ed.*, 2003, **42**, 1483; H. Miyasaka, M. Julve, M. Yamashita and R. Clérac, *Inorg. Chem.*, 2009, **48**, 3420; J. Ferrando-Soria, D. Cangussu, M. Eslava, Y. Journaux, R. Lescouëzec, M. Julve, F. Lloret, J. Pasán, C. Ruiz-Pérez, E. Lhotel, C. Paulsen and E. Pardo, *Chem. Eur. J.*, 2011, **17**, 12482; T. Liu, H. Zheng, S. Kang, Y. Shiota, S. Hayami, M. Mito, O. Sato, K. Yoshizawa, S. Kanegawa and C. Duan, *Nat. Commun.* DOI: 10.1038/ncomms3826.
- 5 For reviews concerning the “second era” of SMMs, see: C. J. Milios and R. E. Winpenny, *Struct. Bond.*, 2014, DOI: 10.1007/430_2014_149; D. N. Woodruff and R. E. P. Winpenny, R. A. Layfield, *Chem. Rev.* 2013, **113**, 5110; P. Zhang, Y.-N. Guo and J. Tang, *Coord. Chem. Rev.*, 2013, **257**, 1728; H. L. C. Feltham and S. Brooker, *Coord. Chem. Rev.*, 2014, **276**, 1; J. D. Rinehart and J. R. Long, *Chem. Sci.*, 2011, **2**, 2078; N. Magnani, *Int. J. Quantum Chem.*, 2014, **114**, 755.
 - 6 R. J. Blagg, L. Ungur, F. Tuna, J. Speak, P. Comar, D. Collison, W. Wernsdorfer, E. J. L. McInnes, L. F. Chibotaru and R. E. P. Winpenny, *Nat. Chem.*, 2013, **5**, 673; C. R. Ganivet, B. Ballesteros, G. de la Torre, J. M. Clemente-Juan, E. Coronado and T. Torres, *Chem. Eur. J.*, 2013, **19**, 1457; M. Gonidec, R. Biagi, V. Corradini, F. Moro, V. De. Renzi, U. Pennino, D. Summa, L. Muccioli, C. Zannoni, D. B. Amabilino and J. Veciana, *J. Am. Chem. Soc.* 2011, **133**, 6603.
 - 7 E. Lucaccini, L. Sorace, M. Perfetti, J. -P. Costes and R. Sessoli, *Chem. Commun.* 2014, **50**, 1648.
 - 8 A. B. Canaj, D. I. Tzimopoulos, A. Philippidis, G. E. Kostakis and C. J. Milios, *Inorg. Chem.*, 2012, **51**, 10461.
 - 9 G. M. Sheldrick, *Acta Crystallogr.* **2008**, *A64*, 112–122.
 - 10 R. A. Coxall, S. G. Harris, D. K. Henderson, S. Parsons, P. A. Tasker and R. E. P. Winpenny, *J. Chem. Soc., Dalton Trans.*, 2000, 2349.
 - 11 I.D. Brown and D. Altermatt, *Acta Crystallogr., B*, 1985, **41**, 244; H.H. Thorpe, *Inorg. Chem.*, 1992, **31**, 1585.
 - 12 M. Llunell, D. Casanova, J. Girera, P. Alemany and S. Alvarez, SHAPE, version 2.0, Barcelona, Spain 2010.
 - 13 M. Wang, D.-Q. Yuan, C.-B. Ma, M.-J. Yuan, M.-Q. Hu, N. Li, H. Chen, C.-N. Chen and Q.-T. Liu, *Dalton Trans.*, 2010, **39**, 7276; G. Rigaux, R. Inglis, S. Morrison, A. Prescimone, C. Cadiou, M. Evangelisti and E. K. Brechin, *Dalton Trans.*, 2010, **40**, 4797.
 - 14 N. F. Chilton, R. P. Anderson, L. D. Turner, A. Soncini and K. S. Murray, *J. Comput. Chem.*, 2013, **34**, 1164.
 - 15 H. Miyasaka, R. Clérac, T. Ishii, H.-C. Chang, S. Kitagawa and M. Yamashita, *J. Chem. Soc., Dalton Trans.*, 2002, 1528; Y. Sato, H. Miyasaka, N. Matsumoto and H. Okawa, *Inorg.*

- Chim. Acta*, 1996, **247**, 57; H.-L. Shyu, H.-H. Wei and Y. Wang, *Inorg. Chim. Acta*, 1999, **290**, 8; C. J. Milios, C. P. Raptopoulou, A. Terzis, F. Lloret, R. Vicente, S. P. Perlepes and A. Escuer, *Angew. Chem., Int. Ed.*, 2004, **43**, 210.
- 16 C. Benelli, M. Murrie, S. Parsons and R. E. P. Winpenny, *J. Chem. Soc., Dalton Trans.*, 1999, 4125; C. Papatriantafyllopoulou, K. A. Abboud and G. Christou, *Inorg. Chem.*, 2011, **50**, 8959; C. Lampropoulos, T. C. Stamatatos, K. A. Abboud and G. Christou, *Inorg. Chem.*, 2009, **48**, 429; V. Mereacre, Y. Lan, R. Clérac, A. M. Ako, I. J. Hewitt, W. Wernsdorfer, G. Buth, C. E. Anson and A. K. Powell, *Inorg. Chem.*, 2010, **49**, 5293.
- 17 S. K. Langley, N. F. Chilton, L. Ungur, B. Moubaraki, L. F. Chibotaru and K. S. Murray, *Inorg. Chem.*, 2012, **51**, 11873; G. Cucinotta, M. Perfetti, J. Luzon, M. Etienne, P.-E. Car, A. Caneschi, G. Calvez, K. Bernot, and Roberta Sessoli, *Angew. Chem. Int. Ed.*, 2012, **51**, 1606; Y.-N. Guo, G.-F. Xu, W. Wernsdorfer, L. Ungur, Y. Guo, J. Tang, H.-J. Zhang, L. F. Chibotaru and A. K. Powell, *J. Am. Chem. Soc.*, 2011, **133**, 11948; N. F. Chilton, S. K. Langley, B. Moubaraki, A. Soncini, S. R. Batten and K. S. Murray, *Chem. Sci.*, 2013, **4**, 1719; F. Tuna, C. A. Smith, M. Bodensteiner, L. Ungur, L. F. Chibotaru, E. J. L. McInnes, R. E. P. Winpenny, D. Collison and R. A. Layfield, *Angew. Chem. Int. Ed.*, 2012, **51**, 6976.
- 18 N. F. Chilton, D. Collison, E. J. L. McInnes, R. E. P. Winpenny and A. Soncini, *Nature Commun.*, 2013, **4**, 2551. a